Science of the Total Environment 832 (2022) 155045

Contents lists available at ScienceDirect

Science of the Total Environment

journal homepage: www.elsevier.com/locate/scitotenv

Dramatic decrease of secondary organic aerosol formation potential in Beijing: Important contribution from reduction of coal combustion emission

Jun Liu [a,c], Biwu Chu [a,b,c,*], Yongcheng Jia [a,c], Qing Cao [a,c], Hong Zhang [a,d,e], Tianzeng Chen [a], Qingxin Ma [a,b,c], Jinzhu Ma [a,b,c], Yonghong Wang [a], Peng Zhang [a], Hong He [a,b,c,*]

[a] State Key Joint Laboratory of Environment Simulation and Pollution Control, Research Center for Eco-Environmental Sciences, Chinese Academy of Sciences, Beijing 100085, China
[b] Center for Excellence in Regional Atmospheric Environment, Institute of Urban Environment, Chinese Academy of Sciences, Xiamen 361021, China
[c] University of Chinese Academy of Sciences, Beijing 100049, China
[d] Beijing Key Lab for Source Control Technology of Water Pollution, College of Environmental Science and Engineering, Beijing Forestry University, Beijing 100083, China
[e] Engineering Research Center for Water Pollution Source Control & Eco-remediation, College of Environmental Science and Engineering, Beijing Forestry University, Beijing 100083, China

HIGHLIGHTS

- SOA formation potential (SOAFP) in urban Beijing was measured using oxidation flow reactor (OFR).
- Causes for the dramatic decrease of SOAFP in two consecutive winters were investigated.
- Emission reduction from coal combustion is critical to significant reduction in SOAFP.
- Transition of "coal-to-gas" and "coal-to-electricity" dominated the emission reduction from coal combustion.

GRAPHICAL ABSTRACT

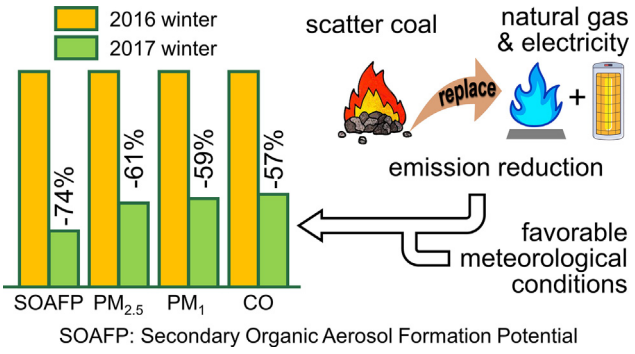

ARTICLE INFO

Editor: Hai Guo

Keywords:
SOA formation potential
Twin-OFRs
Coal-to-gas
Urban area
Emission reduction

ABSTRACT

Secondary organic aerosol (SOA) formation originating from the emission of anthropogenic volatile organic compounds (VOCs) makes a significant contribution to fine particulate matter ($PM_{2.5}$) pollution in urban areas. Investigation on the SOA formation potential (SOAFP) can help us understand the contribution of different sources to SOA formation. To characterize the SOAFP of ambient air from anthropogenic VOCs in the urban area of Beijing, field observation was implemented using a twin oxidation flow reactor (Twin-OFRs) system in the winters of 2016 and 2017. Compared to the winter of 2016, the seasonal-average SOAFP in the winter of 2017 was found to decrease by about 74% (18.6 to 4.9 μg/m^3), which is more than that of PM_1 (59%, 48.7 to 20.2 μg/m^3), $PM_{2.5}$ (61%, 114.4 to 44.8 μg/m^3) and CO (57%, 2.1 to 0.9 mg/m^3) that mainly comes from the combustion of fossil fuels, suggesting complex affecting factors on SOAFP. The results of wind decomposition mathematical modeling showed that anthropogenic factors and favorable meteorological conditions both contributed significantly to the decrease in SOAFP. The reduction of emissions from scatter coal combustion, which is the key VOCs source for SOAFP, is probably the most important anthropogenic factor affecting SOAFP. In the winter of 2016, the ratio of benzene to toluene is 1.45 that was close to 1.54 representing coal combustion emission; however, it decreased dramatically to 1.05 in the winter of 2017, suggesting considerable reduction of VOC emissions from scatter coal combustion in the latter year due to the coal-to-gas transition in Beijing and surrounding regions. The SOAFP measured in this study considers all ambient VOCs that can react with OH radical, providing another representative method for estimating it. These results could be

* Corresponding authors at: State Key Joint Laboratory of Environment Simulation and Pollution Control, Research Center for Eco-Environmental Sciences, Chinese Academy of Sciences, Beijing 100085, China.
E-mail addresses: bwchu@rcees.ac.cn (B. Chu), honghe@rcees.ac.cn (H. He).

http://dx.doi.org/10.1016/j.scitotenv.2022.155045
Received 28 January 2022; Received in revised form 23 March 2022; Accepted 1 April 2022
Available online 8 April 2022

beneficial to understanding the factors driving SOAFP and its contribution to $PM_{2.5}$, especially in regions with high-intensity anthropogenic emissions.

Synopsis: This study reported the sharp decline of secondary organic aerosol formation potential (SOAFP) between two consecutive winters in Beijing and analyzed the reasons.

1. Introduction

Frequently, haze characterized by high mass concentrations of fine particulate matter ($PM_{2.5}$) in developing countries has unfavorable effects on air quality, human health, and regional and global climates (Hallquist et al., 2009; Nel, 2005). In China, particulate matter pollution has also been a severe environmental problem for a long time (Guo et al., 2021; Guo et al., 2014). China's Action Plan of Prevention and Control of Air Pollution (Cai et al., 2017) (clean air action hereafter) was implemented in 2013, whose goal was to reduce the annual average particulate matter mass concentration by certain percentages by 2017 compared with 2012: (a) to reduce the PM_{10} mass concentration by more than 10% for national prefecture-level and above cities; (b) to reduce the $PM_{2.5}$ mass concentration by 25%, 20%, and 15% for the Beijing-Tianjin-Hebei (BTH) region, the Yangtze River Delta (YRD) region, and the Pearl River Delta (PRD) region, respectively; (c) to reduce the $PM_{2.5}$ mass concentration to 60 μg/m^3 or less in Beijing.

Reducing coal consumption is certainly the key to air pollution control in China (Zhang et al., 2012). Therefore, an important measure of the clean air action was to limit the proportion of coal consumption in total energy consumption to less than 65% in 2017. Early policy aiming at effectively reducing the coal consumption of energy-intensive industries achieved that goal, then more attention was paid to the dispersed coal consumption in residential and small-scale factories. For example, the "coal-to-gas" action has been implemented in Beijing and surrounding areas since early 2017, which cut down coal use by replacing traditional coal-fired equipment with gas-fired or electric equipment (Wang et al., 2020).

Submicron aerosol (PM_1) is the dominant subset of $PM_{2.5}$ (Sun et al., 2020; Zhang et al., 2017) and is playing an increasingly important role in atmospheric processes. Organic aerosol (OA) is ubiquitous and contributes significantly (20–90%) to PM_1 globally, while it is the least understood component of PM_1 compared to inorganic aerosols (Jimenez et al., 2009; Kanakidou et al., 2005). Secondary organic aerosol (SOA) is generated by the oxidation of volatile organic compounds (VOCs), semivolatile and intermediate volatility compounds (S/IVOCs) and condensation of the low volatility products, and constitutes a considerable fraction of OA (Hu et al., 2021; Robinson et al., 2007; Shrivastava et al., 2017). In urban Beijing, OA always contributes the largest mass concentration to PM_1 in all seasons, more than half of which is SOA (Chen et al., 2020; Xu et al., 2019; Zhao et al., 2019; Zhou et al., 2019). Environmental chamber experiments, which were mainly designed to study atmospheric chemistry, have focused on SOA formation in recent years (Chen et al., 2019a; Chu et al., 2022). The atmospheric oxidation processes of many VOCs can be parameterized effectively based on the results of chamber experiments under limited conditions. However, there is a considerable gap between experiment-based models and actual observations (Hayes et al., 2015), which highlights the importance of investigating SOA formation in ambient air.

In 2007, Kang et al. (2007) released the 1st generation potential aerosol mass (PAM) reactor, a kind of oxidation flow reactor (OFR), which was used to investigate the SOA formation within short residence time. Subsequent researchers (Chu et al., 2016a; Keller and Burtscher, 2012; Lambe et al., 2011; Li et al., 2019b) have been improving on the reactor over the past ten years for better performance. The high concentration of OH radical in the reactor is likely to alter the oxidation pathways of ambient VOCs; however, the oxidation of VOCs and SOA formation are greatly accelerated, and researchers can obtain roughly the same information on yield and composition as environmental experiments in just a few minutes (Bruns et al., 2015; Lambe et al., 2015).

Many OFR experiments have been conducting to study the SOA formation potentials (SOAFP) of different emission sources, such as vehicle exhaust (Liao et al., 2021; Liu et al., 2019b; Saha et al., 2018), biomass burning (Liu et al., 2019a; Ortega et al., 2013), and plant emissions (Palm et al., 2016; Palm et al., 2018). However, few OFR experiments other than our previous work (Chu et al., 2016a; Liu et al., 2018; Liu et al., 2021) were carried out in downtown area to study the SOA formation in real urban atmospheres (Ortega et al., 2016; Sbai et al., 2021). Ortega et al. (2016) deployed an OFR experiment in Los Angeles to characterize the SOA formation of ambient air, concluding that motor vehicles make an important contribution to urban SOA. Our previous study (Liu et al., 2018) found significantly higher SOAFP in urban Beijing than that of Los Angeles, which suggested that there may be considerable differences in the VOC concentrations between the two cities. Sbai et al. (2021) conducted the first field observation with an OFR to study the SOAFP of ambient air in an urban area of Lyon, and a higher SOAFP than that of Beijing and Los Angeles was observed.

Despite the availability of knowledge on SOAFP over short periods or specific haze events, there has been no study investigating year-to-year SOAFP changes as far as we know. Therefore, field observation using OFR from the winter of 2016 to the winter of 2017 was performed in this study. The contribution of various emission sources such as coal combustion to the variation in SOAFP at different pollution levels was evaluated. Meanwhile, the relative contributions of meteorological conditions and anthropogenic factors to the change in SOAFP in the winter of 2017 were also investigated.

2. Experimental section

2.1. Sampling setup

Three sampling experiments based on Twin-OFRs system were deployed during different periods at a typical urban site in the Research Center for Eco-Environmental Sciences (RCEES, 40.01°N, 116.35°E) located between the north 4th and 5th Ring Roads in Beijing, China. These two discontinuous sampling periods were during the winter of 2016 (2016.12.10–2017.01.19, N = 472 h) and the winter of 2017 (2017.12.04–2018.01.16, N = 738 h). Meanwhile, the sampling was intermittent due to instrument maintenance and repair. Detailed information about the Twin-OFRs utilized can be found in our previous works (Chu et al., 2016a; Liu et al., 2018; Liu et al., 2021).

Surface $PM_{2.5}$, NO_2, CO, SO_2 and O_3 concentrations were obtained in a state-controlled air sampling site, i.e., the National Olympic Sports Center (NOSC, 39.98°N, 116.40°E) station, where $PM_{2.5}$, NO_2, CO, SO_2 and O_3 concentrations were continuously measured. The two stations are both located between the north 4th and 5th Ring Roads in Beijing, while the NOSC station is located 5 km southeast of RCEES station.

2.2. Twin-OFRs setup

The twin-OFRs consist of two stainless steel cylinder reactors coated on the inside with FEP film as shown in Fig. 1. Each reactor is equipped with four 254 nm UV lamps that are turned on in one reactor (active reactor) and turned off in the other reactor (bypass reactor). The active and bypass reactors are switched back and forth every 20–30 min. There is continuous circulating water through the interlayer of the two reactors to keep the inner temperature around 25 °C. The relative humidity (RH) in the two reactors was always controlled in the range of 20%–40%, 0.4%–0.8% water mixing ratio during all measurement periods. As the bulk of OFR

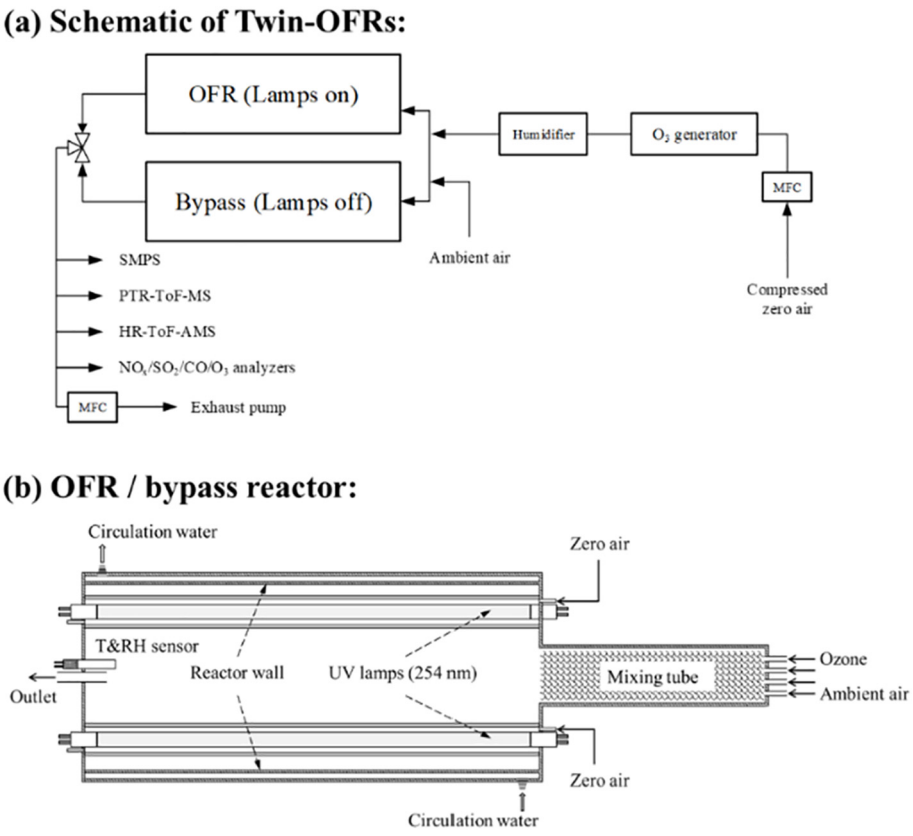

Fig. 1. (a) Schematic of Twin-OFRs system, (b) Structure of OFR/bypass reactor.

applications, this study also concentrated on simulating daytime atmospheric oxidative processes, therefore, OH radicals were chosen as the main oxidant. OH radical is produced inside the active reactor by irradiating humidified O_3, which can oxidize a variety of VOCs into SOA. The OH concentration in the reactor can reach values 4 orders of magnitude higher than those in the atmosphere, which is equivalent to several weeks of OH exposure in the real atmosphere.

SOAFP is the maximum mass concentration of SOA generated by oxidation of VOCs, which is calculated as the difference in the total OA concentrations in the outlets of the two reactors: SOAFP = $OA_{active\ reactor} - OA_{bypass\ reactor}$. The sampling loss of particles and precursors is considered when calculating the SOAFP (Liu et al., 2021). OH exposure is the integral of OH radical concentration and the average residence time in the OFR reactor, according to our experience in our previous studies, it is fixed at about 3 days of atmospheric aging assuming an average OH concentration of 1.5×10^6 molecules/cm^3 to maximize the SOA formation in the reactor. The effect of fluctuations in OH exposure on the estimation of SOAFP was evaluated to be within a reasonable range of deviation (Liu et al., 2021). Low-NO_x conditions in the OFR due to the addition of high concentrations of O_3 could lead to overestimated SOA yield and SOAFP (Eluri et al., 2018; Peng and Jimenez, 2017). In this study, the influence of NO_x on the SOA yield is not the principal focus, while the main goal is to study the relative change in SOAFP in different years.

2.3. Instruments and data analysis

The PM_1 was measured by a high-resolution time-of-flight aerosol mass spectrometer (Aerodyne, hereafter AMS) and a scanning mobility particle sizer (SMPS, TSI Inc., model 3082 with long DMA and 3776 CPC). For AMS, the concentrations of OA, sulfate, nitrate, ammonium, and chloride, as well as the elemental composition of the OA, were measured every 3 min. The measured data were recorded as the 2-min average in "V mode" and 1-min average in "W mode". Every month, the ionization efficiency was calibrated with 300 nm monodisperse, dried ammonium nitrate particles. The relative ionization efficiency for ammonium (RIE-NH_4) varied between 3.8 and 4.1 during the sampling period. The collection efficiency (CE) was assumed to be 0.5 during the whole sampling period. AMS data analysis was performed using Igor Pro 6.37 (Wavemetrics, USA), Squirrel 1.57, and PIKA 1.16. The elemental analysis of OA, including oxygen to carbon ratio (O/C) and hydrogen to carbon ratio (H/C), was performed using the "improved-ambient" method developed by Canagaratna et al. (2015). The density of PM_1 was estimated using the following equation (Li et al., 2018; Zhao et al., 2017):

$$\rho_m = \frac{[NO_3^-] + [SO_4^{2-}] + [NH_4^+] + [Cl^-] + [OA]}{\frac{[NO_3^-]+[SO_4^{2-}]+[NH_4^+]}{1.75} + \frac{[Cl^-]}{1.52} + \frac{[OA]}{1.2}}$$

where the densities are 1.75 g/cm^3 for ammonium nitrate and ammonium sulfate, 1.52 g/cm^3 for ammonium chloride, 1.2 g/cm^3 for OA. The SMPS data was used to measure the PM_1 mass concentration with 5 min resolution. The mass concentration of PM_1 was calculated based on the volume concentration from SMPS and the density estimated from the component of PM_1 as show above. The PM_1 mass concentration measured by AMS and SMPS is in good agreement (slope = 0.98 and r^2 = 0.92, see Fig. S1).

The NO_x, CO, SO_2 and O_3 levels at the inlet and outlet of the two reactors were monitored by gas analyzers (model 42i, 48i, 43i and 49i, Thermo Fisher) with 1 min resolution. NO_x, CO and SO_2 analyzers were calibrated every two weeks using the multi-gas calibrator (model 146i, Thermo Fisher), and O_3 analyzer was calibrated at same intervals using O_3 calibrator (model 49i-PS, Thermo Fisher). A proton transfer reaction time-of-flight mass spectrometer (PTR-ToF-MS, Ionicon, here after PTR) was used to measure concentrations of some VOCs with H_3O^+ as the primary reaction ion. The operating pressure, temperature, voltage, and consequent E/N (E: electric field strength, N: number density of the gas) in the drift tube are 3.8 mbar, 60 °C, 993 V and ~132 Td, respectively. The PTR was operated

at a flow rate of 100 ml/min and a time resolution of 5 min. The PTR-MS Viewer software (version 3.1.0.31) was used to analyze the data. A 57-component VOCs gas standard was diluted by gas dilution calibrator (model 2010, Sabio Environmental) to calibrate the PTR.

3. Results and discussion

3.1. Substantial decline in pollutant concentrations in winter from 2016 to 2017

The air quality in China is getting better and better after the implementation of the clean air action, especially in the BTH region. In recent years, the largest decline in the mass concentration of pollutants in Beijing occurred between 2016 and 2017, as shown in Figs. S2–S3, especially in winter. Compared to the winter of 2016, the mass concentrations of $PM_{2.5}$, NO_2, SO_2 and CO in the winter of 2017 were reduced by 61%, 37%, 52% and 57%, respectively, as shown in Fig. 2. Especially for $PM_{2.5}$ and CO, the levels became close to or even lower than those in summer of 2017, as shown in Table S1. The concentrations of VOCs also decreased. For example, the aromatic hydrocarbons with 6–9 carbons (C6–C9 aromatics), which are regarded as an indicator of the anthropogenic precursor VOCs in this study, decreased by 46% during the same period. Compared to the winter of 2016, the mass concentration of PM_1 in the winter of 2017 dropped by 58.5% from 48.7 to 20.2 μg/m^3, with more detail on time variations shown in Figs. S4–S5, which is slightly lower than the reduction in $PM_{2.5}$. As the components of PM_1, the mass concentrations of OA, nitrate, sulfate, ammonium, and chloride declined by 59%, 57%, 62%, 58% and 40%, respectively. OA constitutes the majority of the PM_1 and accounts for 41.5% and 41.0% in the winters of 2016 and 2017, respectively, as shown in Figs. S4–S5. Compared to the winter of 2016, all these pollutants decreased dramatically in the winter of 2017. In particular, the SOAFP was found to drop by 74% from 18.6 to 4.9 μg/m^3, which is higher than the drop in $PM_{2.5}$.

3.2. Contribution from changes in meteorological conditions

Meteorological conditions were found to make considerable contributions to the improvement in the air quality in China (Ma et al., 2021; Zhang et al., 2019b; Zhang et al., 2019c). From 2013 to 2017, about 10% of national $PM_{2.5}$ reduction can be ascribed to meteorological conditions; in particular, it accounted for about 15% for the BTH region (Zhai et al., 2019; Zhang et al., 2019b). In this study, a mathematical model (Li et al., 2014; Song et al., 2021) based on a wind decomposition method was used to quantify the contributions of meteorological conditions (wind speed, wind direction, temperature, and relative humidity) and anthropogenic factors to the changes in the concentrations of CO, $PM_{2.5}$ and SOAFP. This model is based on the mathematical expectation calculated from the frequency distribution of pollutant concentrations associated with the meteorological conditions, which is described in detail in Section S1 in the supplemental material. CO and $PM_{2.5}$ decrease by 57% (2.1 to 0.9 mg/m^3) and 61% (114.4 to 44.8 μg/m^3) in winter from 2016 to 2017, respectively. The decomposition results shown that meteorological conditions contributed about 50% to the reduction of CO and $PM_{2.5}$, which are 0.6 mg/m^3 and 35 μg/m^3, respectively, as shown in Fig. 3a. It is consistent with a previous model study reporting that favorable meteorological conditions played a critical role in the air quality improvement in the winter of 2017 (Zhang et al., 2019b). Due to the simple setup in the mathematical model, there is still substantial residue in the decomposition results, indicating significant contributions from unconsidered factors such as precipitation, atmospheric pressure, radiation etc. For the increase of O_3 in the winter of 2017, meteorological factors played a dominant role, in which the reduction of RH may relate to a favorable atmospheric condition for O_3 accumulation, such as more solar irradiation (Camalier et al., 2007), less sink for radicals and related low-volatility intermediate species (Jia and Xu, 2014; Li et al., 2019a) and so on. Among meteorological factors, decreasing RH also has a dominant influence on the decrease of $PM_{2.5}$, CO and SOAFP, according to the decomposition of meteorological parameters shown in Fig. 3b. Lower RH was usually accompanied by favorable atmospheric diffusion conditions. This is consistent with the marked variation in RH between the two years, as shown in Fig. 3c, and the crucial role of RH in haze formation in northern China, which has been reported widely in previous studies (Chen et al., 2020; Zhai et al., 2019). In addition, more solar irradiation (Camalier et al., 2007) and less radical loss (Park et al., 2008) under lower RH condition would promote the photochemical oxidation of VOCs, which led to more SOA formation and less SOAFP. Increasing wind speed in 2017 compared to 2016 contributed less to the reduction of SOAFP than RH, while the influence of temperature is estimated to be small.

3.3. Contribution from the decrease in emission from anthropogenic sources

The non-meteorological factors are those control measures that changes emission from anthropogenic sources, which is another important reason for the reduction in SOAFP. Anthropogenic VOC emissions from solvent use, industrial processes, transportation, and domestic combustion contribute most of the SOA formation in Beijing and the surrounding area (Wu et al., 2017). According to the estimate of Wu and Xie (2017), aromatic

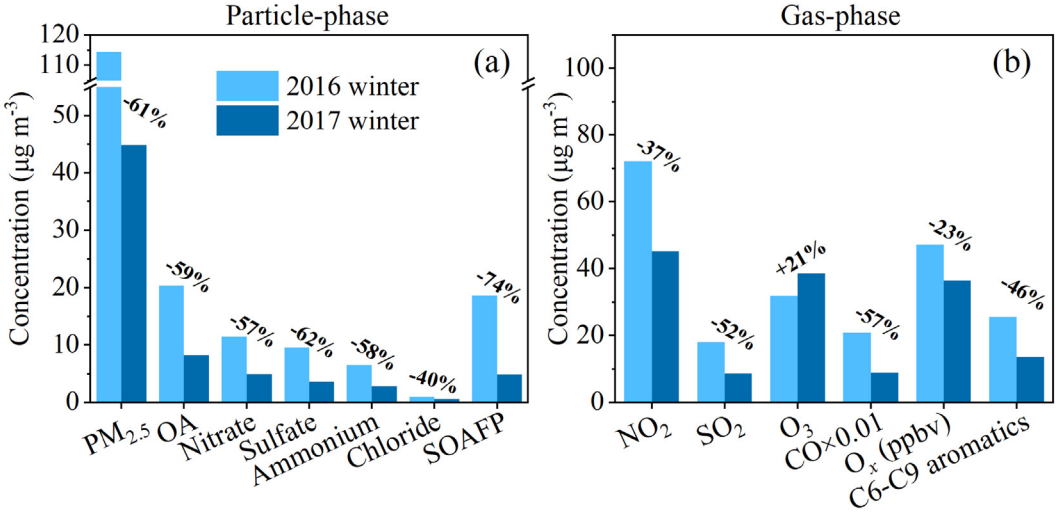

Fig. 2. Particle-phase (a) and gas-phase (b) concentrations of pollutants in the winters of 2016 and 2017 in Beijing. The concentrations of $PM_{2.5}$, NO_2, CO, SO_2 and O_3 were obtained in a state-controlled air sampling site (NOSC). PM_1 and its components (OA, nitrate, sulfate, ammonium, and chloride reduce) were measured in the RCEES station.

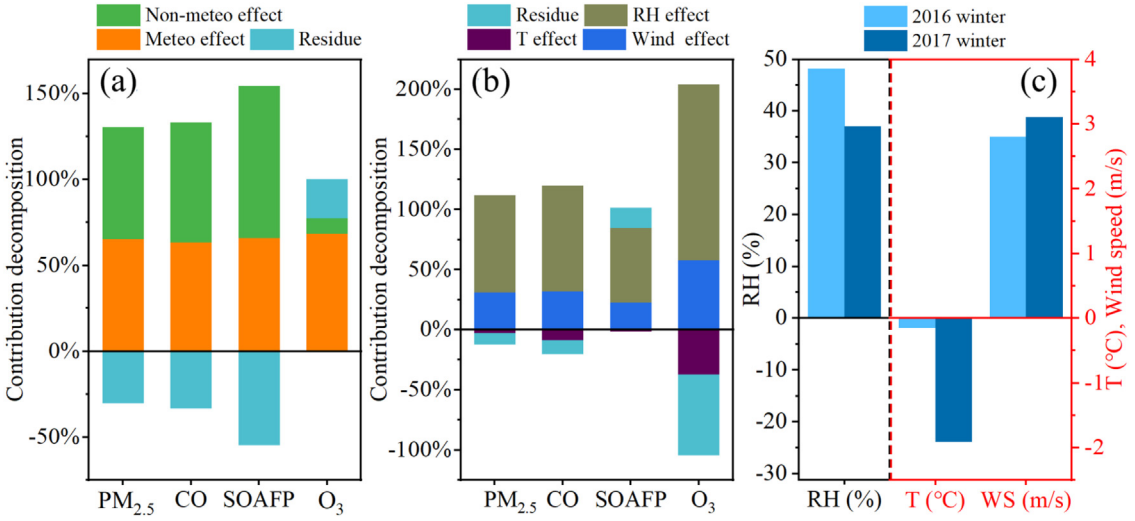

Fig. 3. Relative contribution of meteorological and non-meteorological factors to SOAFP, CO and $PM_{2.5}$ (a); Factor decomposition of the meteorological conditions (b); Temperature (T), relative humidity (RH) and wind speed (WS) in the winters of 2016 and 2017 in Beijing (c).

hydrocarbons contribute 68.6% of the SOAFP in China based on a speciated anthropogenic VOC emission inventory. Moreover, this contribution may reach more than 90% in Beijing (Li et al., 2020; Zhang et al., 2021). In this study, the concentration of C6–C9 aromatic VOCs decreased by 46%, which is close to the reported reduction in ambient VOCs concentrations by 52% during the same periods (Shi et al., 2020). The significant decrease in VOC precursors is consistent with the decrease in SOAFP, although the decrease ratio of these VOCs is lower than that of SOAFP. This may be partly due to the fact that not all precursor VOCs can be identified, so there are probably unidentified precursor VOCs with higher reduction ratios than that of C6–C9 aromatics. Another reason would be changes in the atmospheric oxidation conditions, which will be discussed later in the next section.

Emissions from heating systems in winter are one of the main pollutant sources in north China (Liu et al., 2016; Zhang et al., 2016). Coal burning was the main heating method in the winter in Beijing and surrounding areas before 2017, which has been gradually replaced by natural gas since early 2017 (Wang et al., 2020). Emission from coal combustion not only contributed most of the CO and SO_2 emission in China (Sun et al., 2018), but also substantially affected the anthropogenic VOC emission (Wu et al., 2017). Rigorous measures to control dispersed coal use resulted in an 892.1 Gg (16.2%) decrease in primary CO emission over "2 + 26" cities in the heating period of 2017 compared to the same period of 2016 (Wang et al., 2020). This reduction ratio is clearly lower than the observed reduction in CO shown in Fig. S7, which confirmed the considerable contribution from beneficial meteorological conditions in the winter of 2017.

Rigorous measures controlling dispersed coal use were found to be the main reason for the reduction in VOC precursors in the winter of 2017. The ratio of benzene to toluene has been widely used to characterize the emissions of VOCs from coal combustion and vehicle exhaust. The upper and lower boundaries of this ratio (about 1.54 and 0.59) represent coal combustion and vehicle emission sources, respectively, as sole contributors (Liu et al., 2017). In the winter of 2016, this ratio was 1.45, which is close to the upper limit, suggesting that the dominant emission sources were VOCs from coal combustion, as shown in Fig. 4; and the lower ratio of 1.05 in the winter of 2017 indicates that coal consumption was significantly reduced compared to the winter of 2016. Meanwhile, the lower decline ratio of NO_2 (37%) in the winter of 2017 than that of SO_2 (52%) compared with the winter of 2016 also supports the reduction in scattered residential coal burning, since it contributed a lot of SO_2 emission while NO_x mainly comes from other sources, such as vehicles (Li et al., 2017).

Similarly, Shi et al. (2020) reported that although coal burning constituted 27% of ambient VOCs, it contributed about 40% on average to the SOAFP in the winters of 2016 and 2017 based on the explicit SOA yield models and corrected VOCs emission inventory. According to the source apportionment of VOCs, the estimated SOAFP decreased by about 64% in the winter of 2017, of which coal burning accounted for 55% of the reduction (Shi et al., 2020). Instead of estimating SOAFP by considering the combined effects of more than 100 known identified VOCs, the SOAFP measured in this study can provide another representative method which considers all ambient VOCs that can react with OH radical in the OFR and corresponds well to the reduction in VOC emission from key anthropogenic sources.

3.4. Contribution from changes in atmospheric oxidation conditions

In addition to decreasing the direct emission of VOCs, the dramatic decline in pollution levels may lead to an increase in irradiation and more intense photochemical reactions in the ambient air, promoting the conversion of VOCs (Liu et al., 2021). The greater reduction ratio for SOAFP than that

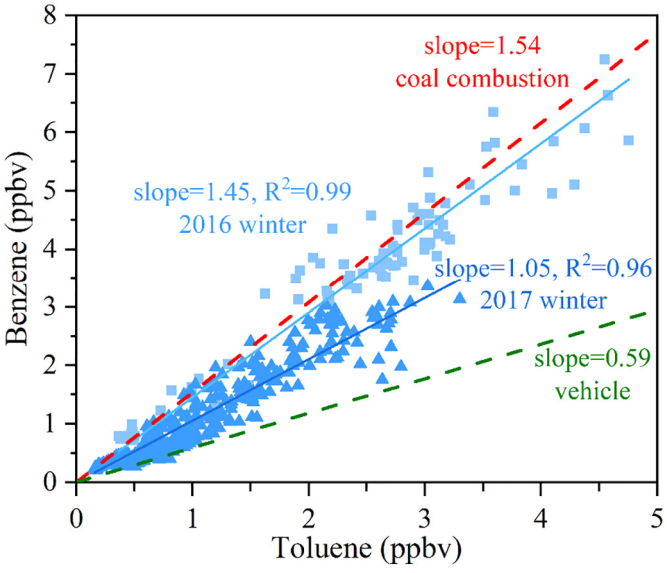

Fig. 4. Ratio of benzene to toluene in the winters of 2016 and 2017.

for OA in the winter of 2017, as shown in Fig. 2, confirmed that a higher proportion of precursor VOCs was converted to SOA. Besides, the decrease in other air pollutants such as SO_2 and NO_2 may also have important influences on OA pollution under complex pollution conditions (Chu et al., 2016b; Xu et al., 2020; Zhang et al., 2019a). The acid catalytic effects of SO_2 and its oxidation products on SOA formation have been widely reported (Chen et al., 2019b; Liggio et al., 2007), while NO_2 can affect SOA formation by participating in the formation of organic nitrates (Ma et al., 2018). NO_2 is also an important oxidant under high NH_3 and NO_2 concentrations (Huang et al., 2014) and can change the formation pathway of O_3 and consequent VOC oxidation. As an indicator of atmospheric photochemical activity, odd oxygen ($O_x = NO_2 + O_3$) is composed of predominantly NO_2 in this study, which decreased by 23% in the winter of 2017. In addition, the lower aqueous water content with lighter pollution levels and lower RH in 2017 is not beneficial to the formation of aqueous OA (Xu et al., 2017), which may also affect the SOAFP. These factors could bring about the lower reduction ratio for VOCs than that for OA in the winter of 2017. Due to the difficulty in quantifying the atmospheric oxidation capacity and the complex relationship between it and SOAFP, its influence on SOAFP is difficult to be quantified.

4. Conclusions and atmospheric implications

In our previous work, the SOAFP at different pollution level with different precursor concentrations and atmospheric oxidation conditions were characterized. This study further investigates the effects of these factors as well as meteorological conditions on the interannual variation of SOAFP between the winters of 2016 and 2017. The dramatic reduction of SOAFP in the winter of 2017 compared to the winter of 2016 was observed, which is found to be driven by the reduction in emissions and the favorable meteorological conditions according to the results of wind decomposition model. The reduction in VOCs from coal combustion was found to be the most important anthropogenic factor contributing to the decrease in the SOAFP in the winter of 2017. The ratio of benzene to toluene in the winter of 2016 (1.45) was close to 1.54, which represents emission from coal combustion, indicating that VOC emissions from coal combustion dominated in the winter of 2016 in Beijing. However, the strikingly lower ratio in the winter of 2017 (1.05) indicates a significant reduction in coal consumption compared to the winter of 2016 due to the coal-to-gas transition in Beijing and surrounding regions, which is also consistent to the estimated variation of VOCs emission from scatter coal burning. Besides the reduction in VOC emissions, the favorable meteorological conditions in the winter of 2017 also significantly promoted the decline in SOAFP, among which decreasing RH dominated the contributions. In the "2 + 26" cities including Beijing, the observed reduction in CO concentrations was significantly greater than that of primary CO emissions, which also suggest the significant effect of favorable meteorological conditions on the improvement of air quality in 2017. Moreover, coal combustion contributed most of the CO emissions in China, and similar reductions in CO and precursor VOCs were observed in this study. Although there is a lack of data on precursor VOCs in the surrounding areas of Beijing, the SOAFP in related regions was likely to decrease significantly as inferred from the observed reduction in CO concentrations. Overall, based on the available evidence, the decline in emissions from coal combustion and decreased RH were the principal reasons for the sharp drop in SOAFP in the winter of 2017.

Many strict measures for controlling pollutants have been implemented by the Chinese government, and remarkable phased goals have been achieved. Among these measures, the reduction in coal combustion emission helped to decrease not only ambient SO_2 and CO, but also the VOCs and consequent SOA formation. Meanwhile, the atmospheric oxidation capacity may change with the improvement of air quality, further affecting the secondary aerosol formation. SOAFP can provide a representative viewpoint which considers all ambient VOCs that can react with OH radical in the OFR. The continuous measurement of SOAFP from ambient air may provide helpful insights for emission-reduction strategies and assessment of the effectiveness of OA pollution control.

CRediT authorship contribution statement

Jun Liu: Conceptualization, Investigation, Writing - original draft, Writing - review & editing. **Biwu Chu:** Conceptualization, Methodology, Writing - review & editing. **Yongcheng Jia:** Software, Formal analysis. **Qing Cao:** Data curation, Investigation. **Hong Zhang:** Software, Investigation. **Tianzeng Chen:** Writing - review & editing, formal analysis. **Qingxin Ma:** Validation. Formal analysis. **Jinzhu Ma:** Formal analysis. **Yonghong Wang:** Writing - review & editing. **Peng Zhang:** Validation. **Hong He:** Conceptualization, Supervision, Funding acquisition.

Declaration of competing interest

The authors declare that they have no known competing financial interests or personal relationships that could have appeared to influence the work reported in this paper.

Acknowledgments

This work was financially supported by the National Natural Science Foundation of China (41877304, 22188102, 22122610 and 22006152) and the Youth Innovation Promotion Association, CAS (2018060). We also thank Ms. Qingcai Feng for her great help in editing this paper and Dr. Xiaolei Bao for providing us the PTR-MS and helpful support.

Appendix A. Supplementary data

Supplementary data to this article can be found online at https://doi.org/10.1016/j.scitotenv.2022.155045.

References

Bruns, E.A., El Haddad, I., Keller, A., Klein, F., Kumar, N.K., Pieber, S.M., Corbin, J.C., Slowik, J.G., Brune, W.H., Baltensperger, U., Prevot, A.S.H., 2015. Inter-comparison of laboratory smog chamber and flow reactor systems on organic aerosol yield and composition. Atmos. Meas. Tech. 8, 2315–2332.

Cai, S., Wang, Y., Zhao, B., Wang, S., Chang, X., Hao, J., 2017. The impact of the "Air Pollution Prevention and Control Action Plan" on $PM_{2.5}$ concentrations in Jing-Jin-Ji region during 2012–2020. Sci. Total Environ. 580, 197–209.

Camalier, L., Cox, W., Dolwick, P., 2007. The effects of meteorology on ozone in urban areas and their use in assessing ozone trends. Atmos. Environ. 41, 7127–7137.

Canagaratna, M.R., Jimenez, J.L., Kroll, J.H., Chen, Q., Kessler, S.H., Massoli, P., Hildebrandt, Ruiz L., Fortner, E., Williams, L.R., Wilson, K.R., Surratt, J.D., Donahue, N.M., Jayne, J.T., Worsnop, D.R., 2015. Elemental ratio measurements of organic compounds using aerosol mass spectrometry: characterization, improved calibration, and implications. Atmos. Chem. Phys. 15, 253–272.

Chen, T.Z., Liu, Y.C., Liu, C.G., Liu, J., Chu, B.W., He, H., 2019a. Important role of aromatic hydrocarbons in SOA formation from unburned gasoline vapor. Atmos. Environ. 201, 101–109.

Chen, T.Z., Liu, Y.C., Ma, Q.X., Chu, B.W., Zhang, P., Liu, C.G., Liu, J., He, H., 2019b. Significant source of secondary aerosol: formation from gasoline evaporative emissions in the presence of SO_2 and NH_3. Atmos. Chem. Phys. 19, 8063–8081.

Chen, T., Liu, J., Liu, Y., Ma, Q., Ge, Y., Zhong, C., Jiang, H., Chu, B., Zhang, P., Ma, J., Liu, P., Wang, Y., Mu, Y., He, H., 2020. Chemical characterization of submicron aerosol in summertime Beijing: a case study in southern suburbs in 2018. Chemosphere 247, 125918.

Chu, B., Liu, Y., Ma, Q., Ma, J., He, H., Wang, G., Cheng, S., Wang, X., 2016a. Distinct potential aerosol masses under different scenarios of transport at a suburban site of Beijing. J. Environ. Sci. (China) 39, 52–61.

Chu, B.W., Zhang, X., Liu, Y.C., He, H., Sun, Y., Jiang, J.K., Li, J.H., Hao, J.M., 2016b. Synergetic formation of secondary inorganic and organic aerosol: effect of SO_2 and NH_3 on particle formation and growth. Atmos. Chem. Phys. 16, 14219–14230.

Chu, B.W., Chen, T.Z., Liu, Y.C., Ma, Q.X., Mu, Y.J., Wang, Y.H., Ma, J.Z., Zhang, P., Liu, J., Liu, C.S., Gui, H.Q., Hu, R.Z., Hu, B., Wang, X.M., Wang, Y.S., Liu, J.G., Xie, P.H., Chen, J.M., Liu, Q., Jiang, J.K., Li, J.H., He, K.B., Liu, W.Q., Jiang, G.B., Hao, J.M., He, H., 2022. Application of smog chambers in atmospheric process studies. Natl. Sci. Rev. 9, 16.

Eluri, S., Cappa, C.D., Friedman, B., Farmer, D.K., Jathar, S.H., 2018. Modeling the formation and composition of secondary organic aerosol from diesel exhaust using parameterized and semi-explicit chemistry and thermodynamic models. Atmos. Chem. Phys. 18, 13813–13838.

Guo, S., Hu, M., Zamora, M.L., Peng, J.F., Shang, D.J., Zheng, J., Du, Z.F., Wu, Z., Shao, M., Zeng, L.M., Molina, M.J., Zhang, R.Y., 2014. Elucidating severe urban haze formation in China. Proc. Natl. Acad. Sci. U. S. A. 111, 17373–17378.

Guo, B., Wang, X., Pei, L., Su, Y., Zhang, D., Wang, Y., 2021. Identifying the spatiotemporal dynamic of $PM_{2.5}$ concentrations at multiple scales using geographically and temporally weighted regression model across China during 2015–2018. Sci. Total Environ. 751.

Hallquist, M., Wenger, J.C., Baltensperger, U., Rudich, Y., Simpson, D., Claeys, M., Dommen, J., Donahue, N.M., George, C., Goldstein, A.H., Hamilton, J.F., Herrmann, H., Hoffmann, T., Iinuma, Y., Jang, M., Jenkin, M.E., Jimenez, J.L., Kiendler-Scharr, A., Maenhaut, W., McFiggans, G., Mentel, T.F., Monod, A., Prevot, A.S.H., Seinfeld, J.H., Surratt, J.D., Szmigielski, R., Wildt, J., 2009. The formation, properties and impact of secondary organic aerosol: current and emerging issues. Atmos. Chem. Phys. 9, 5155–5236.

Hayes, P.L., Carlton, A.G., Baker, K.R., Ahmadov, R., Washenfelder, R.A., Alvarez, S., Rappengluck, B., Gilman, J.B., Kuster, W.C., de Gouw, J.A., Zotter, P., Prevot, A.S.H., Szidat, S., Kleindienst, T.E., Offenberg, J.H., Ma, P.K., Jimenez, J.L., 2015. Modeling the formation and aging of secondary organic aerosols in Los Angeles during CalNex 2010. Atmos. Chem. Phys. 15, 5773–5801.

Hu, W., Zhou, H., Chen, W., Ye, Y., Pan, T., Wang, Y., Song, W., Zhang, H., Deng, W., Zhu, M., Wang, C., Wu, C., Ye, C., Wang, Z., Yuan, B., Huang, S., Shao, M., Peng, Z., Day, D.A., Campuzano-Jost, P., Lambe, A.T., Worsnop, D.R., Jimenez, J.L., Wang, X., 2021. Oxidation flow reactor results in a chinese megacity emphasize the important contribution of S/IVOCs to ambient SOA formation. Environ. Sci. Technol. https://doi.org/10.1021/acs.est.1c03155.

Huang, X., Song, Y., Zhao, C., Li, M.M., Zhu, T., Zhang, Q., Zhang, X.Y., 2014. Pathways of sulfate enhancement by natural and anthropogenic mineral aerosols in China. J. Geophys. Res.-Atmos. 119, 14165–14179.

Jia, L., Xu, Y., 2014. Effects of relative humidity on ozone and secondary organic aerosol formation from the photooxidation of benzene and ethylbenzene. Aerosol Sci. Technol. 48, 1–12.

Jimenez, J.L., Canagaratna, M.R., Donahue, N.M., Prevot, A.S., Zhang, Q., Kroll, J.H., DeCarlo, P.F., Allan, J.D., Coe, H., Ng, N.L., Aiken, A.C., Docherty, K.S., Ulbrich, I.M., Grieshop, A.P., Robinson, A.L., Duplissy, J., Smith, J.D., Wilson, K.R., Lanz, V.A., Hueglin, C., Sun, Y.L., Tian, J., Laaksonen, A., Raatikainen, T., Rautiainen, J., Vaattovaara, P., Ehn, M., Kulmala, M., Tomlinson, J.M., Collins, D.R., Cubison, M.J., Dunlea, E.J., Huffman, J.A., Onasch, T.B., Alfarra, M.R., Williams, P.I., Bower, K., Kondo, Y., Schneider, J., Drewnick, F., Borrmann, S., Weimer, S., Demerjian, K., Salcedo, D., Cottrell, L., Griffin, R., Takami, A., Miyoshi, T., Hatakeyama, S., Shimono, A., Sun, J.Y., Zhang, Y.M., Dzepina, K., Kimmel, J.R., Sueper, D., Jayne, J.T., Herndon, S.C., Trimborn, A.M., Williams, L.R., Wood, E.C., Middlebrook, A.M., Kolb, C.E., Baltensperger, U., Worsnop, D.R., 2009. Evolution of organic aerosols in the atmosphere. Science 326, 1525–1529.

Kanakidou, M., Seinfeld, J.H., Pandis, S.N., Barnes, I., Dentener, F.J., Facchini, M.C., Van Dingenen, R., Ervens, B., Nenes, A., Nielsen, C.J., Swietlicki, E., Putaud, J.P., Balkanski, Y., Fuzzi, S., Horth, J., Moortgat, G.K., Winterhalter, R., Myhre, C.E.L., Tsigaridis, K., Vignati, E., Stephanou, E.G., Wilson, J., 2005. Organic aerosol and global climate modelling: a review. Atmos. Chem. Phys. 5, 1053–1123.

Kang, E., Root, M.J., Toohey, D.W., Brune, W.H., 2007. Introducing the concept of Potential Aerosol Mass (PAM). Atmos. Chem. Phys. 7, 5727–5744.

Keller, A., Burtscher, H., 2012. A continuous photo-oxidation flow reactor for a defined measurement of the SOA formation potential of wood burning emissions. J. Aerosol Sci. 49, 9–20.

Lambe, A.T., Ahern, A.T., Williams, L.R., Slowik, J.G., Wong, J.P.S., Abbatt, J.P.D., Brune, W.H., Ng, N.L., Wright, J.P., Croasdale, D.R., Worsnop, D.R., Davidovits, P., Onasch, T.B., 2011. Characterization of aerosol photooxidation flow reactors: heterogeneous oxidation, secondary organic aerosol formation and cloud condensation nuclei activity measurements. Atmos. Meas. Tech. 4, 445–461.

Lambe, A.T., Chhabra, P.S., Onasch, T.B., Brune, W.H., Hunter, J.F., Kroll, J.H., Cummings, M.J., Brogan, J.F., Parmar, Y., Worsnop, D.R., Kolb, C.E., Davidovits, P., 2015. Effect of oxidant concentration, exposure time, and seed particles on secondary organic aerosol chemical composition and yield. Atmos. Chem. Phys. 15, 3063–3075.

Li, Y., Lau, A., Wong, A., Fung, J., 2014. Decomposition of the wind and nonwind effects on observed year-to-year air quality variation. J. Geophys. Res.-Atmos. 119, 6207–6220.

Li, M., Liu, H., Geng, G.N., Hong, C.P., Liu, F., Song, Y., Tong, D., Zheng, B., Cui, H.Y., Man, H.Y., Zhang, Q., He, K.B., 2017. Anthropogenic emission inventories in China: a review. Natl. Sci. Rev. 4, 834–866.

Li, K., Chen, L., White, S.J., Zheng, X., Lv, B., Lin, C., Bao, Z., Wu, X., Gao, X., Ying, F., Shen, J., Azzi, M., Cen, K., 2018. Chemical characteristics and sources of PM_1 during the 2016 summer in Hangzhou. Environ. Pollut. 232, 42–54.

Li, K., Jacob, D.J., Liao, H., Shen, L., Zhang, Q., Bates, K.H., 2019a. Anthropogenic drivers of 2013–2017 trends in summer surface ozone in China. Proc. Natl. Acad. Sci. U. S. A. 116, 422–427.

Li, K., Liggio, J., Lee, P., Han, C., Liu, Q.F., Li, S.M., 2019b. Secondary organic aerosol formation from alpha-pinene, alkanes, and oil-sands-related precursors in a new oxidation flow reactor. Atmos. Chem. Phys. 19, 9715–9731.

Li, Q., Su, G., Li, C., Liu, P., Zhao, X., Zhang, C., Sun, X., Mu, Y., Wu, M., Wang, Q., Sun, B., 2020. An investigation into the role of VOCs in SOA and ozone production in Beijing, China. Sci. Total Environ. 720, 137536.

Liao, K., Chen, Q., Liu, Y., Li, Y.J., Lambe, A.T., Zhu, T., Huang, R.J., Zheng, Y., Cheng, X., Miao, R., Huang, G., Khuzestani, R.B., Jia, T., 2021. Secondary organic aerosol formation of fleet vehicle emissions in China: potential seasonality of spatial distributions. Environ. Sci. Technol. 55, 7276–7286.

Liggio, J., Li, S.-M., Brook, J.R., Mihele, C., 2007. Direct polymerization of isoprene and α-pinene on acidic aerosols. Geophys. Res. Lett. 34.

Liu, J., Mauzerall, D.L., Chen, Q., Zhang, Q., Song, Y., Peng, W., Klimont, Z., Qiu, X., Zhang, S., Hu, M., Lin, W., Smith, K.R., Zhu, T., 2016. Air pollutant emissions from chinese households: a major and underappreciated ambient pollution source. Proc. Natl. Acad. Sci. U. S. A. 113, 7756–7761.

Liu, C.T., Ma, Z.B., Mu, Y.J., Liu, J.F., Zhang, C.L., Zhang, Y.Y., Liu, P.F., Zhang, H.X., 2017. The levels, variation characteristics, and sources of atmospheric non-methane hydrocarbon compounds during wintertime in Beijing,China. Atmos. Chem. Phys. 17, 10633–10649.

Liu, J., Chu, B., Chen, T., Liu, C., Wang, L., Bao, X., He, H., 2018. Secondary organic aerosol formation from ambient air at an urban site in Beijing: effects of OH exposure and precursor concentrations. Environ. Sci. Technol. 52, 6834–6841.

Liu, C.G., Liu, J., Liu, Y.C., Chen, T.Z., He, H., 2019a. Secondary organic aerosol formation from the OH-initiated oxidation of guaiacol under different experimental conditions. Atmos. Environ. 207, 30–37.

Liu, T., Zhou, L., Liu, Q., Lee, B.P., Yao, D., Lu, H., Lyu, X., Guo, H., Chan, C.K., 2019b. Secondary organic aerosol formation from urban roadside air in Hong Kong. Environ. Sci. Technol. 53, 3001–3009.

Liu, J., Chu, B., Chen, T., Zhong, C., Liu, C., Ma, Q., Ma, J., Zhang, P., He, H., 2021. Secondary organic aerosol formation potential from ambient air in Beijing: effects of atmospheric oxidation capacity at different pollution levels. Environ. Sci. Technol. 55, 4565–4572.

Ma, J., Chu, B., Liu, J., Liu, Y., Zhang, H., He, H., 2018. NO_x promotion of SO_2 conversion to sulfate: an important mechanism for the occurrence of heavy haze during winter in Beijing. Environ. Pollut. 233, 662–669.

Ma, S., Shao, M., Zhang, Y., Dai, Q., Xie, M., 2021. Sensitivity of $PM_{2.5}$ and O_3 pollution episodes to meteorological factors over the North China Plain. Sci. Total Environ. 792.

Nel, A., 2005. Atmosphere. Air pollution-related illness: effects of particles. Science 308, 804–806.

Ortega, A.M., Day, D.A., Cubison, M.J., Brune, W.H., Bon, D., de Gouw, J.A., Jimenez, J.L., 2013. Secondary organic aerosol formation and primary organic aerosol oxidation from biomass-burning smoke in a flow reactor during FLAME-3. Atmos. Chem. Phys. 13, 11551–11571.

Ortega, A.M., Hayes, P.L., Peng, Z., Palm, B.B., Hu, W.W., Day, D.A., Li, R., Cubison, M.J., Brune, W.H., Graus, M., Warneke, C., Gilman, J.B., Kuster, W.C., de Gouw, J., Gutierrez-Montes, C., Jimenez, J.L., 2016. Real-time measurements of secondary organic aerosol formation and aging from ambient air in an oxidation flow reactor in the Los Angeles area. Atmos. Chem. Phys. 16, 7411–7433.

Palm, B.B., Campuzano-Jost, P., Ortega, A.M., Day, D.A., Kaser, L., Jud, W., Karl, T., Hansel, A., Hunter, J.F., Cross, E.S., Kroll, J.H., Peng, Z., Brune, W.H., Jimenez, J.L., 2016. In situ secondary organic aerosol formation from ambient pine forest air using an oxidation flow reactor. Atmos. Chem. Phys. 16, 2943–2970.

Palm, B.B., de Sa, S.S., Day, D.A., Campuzano-Jost, P., Hu, W.W., Seco, R., Sjostedt, S.J., Park, J.H., Guenther, A.B., Kim, S., Brito, J., Wurm, F., Artaxo, P., Thalman, R., Wang, J., Yee, L.D., Wernis, R., Isaacman-VanWertz, G., Goldstein, A.H., Liu, Y.J., Springston, S.R., Souza, R., Newburn, M.K., Alexander, M.L., Martin, S.T., Jimenez, J.L., 2018. Secondary organic aerosol formation from ambient air in an oxidation flow reactor in central Amazonia. Atmos. Chem. Phys. 18, 467–493.

Park, J.H., Ivanov, A.V., Molina, M.J., 2008. Effect of relative humidity on OH uptake by surfaces of atmospheric importance. J. Phys. Chem. A 112, 6968–6977.

Peng, Z., Jimenez, J.L., 2017. Modeling of the chemistry in oxidation flow reactors with high initial NO. Atmos. Chem. Phys. 17, 11991–12010.

Robinson, A.L., Donahue, N.M., Shrivastava, M.K., Weitkamp, E.A., Sage, A.M., Grieshop, A.P., Lane, T.E., Pierce, J.R., Pandis, S.N., 2007. Rethinking organic aerosols: semivolatile emissions and photochemical aging. Science 315, 1259–1262.

Saha, P.K., Reece, S.M., Grieshop, A.P., 2018. Seasonally varying secondary organic aerosol formation from in-situ oxidation of near-highway air. Environ. Sci. Technol. 52, 7192–7202.

Sbai, S.E., Li, C., Boreave, A., Charbonnel, N., Perrier, S., Vernoux, P., Bentayeb, F., George, C., Gil, S., 2021. Atmospheric photochemistry and secondary aerosol formation of urban air in Lyon,France. J. Environ. Sci. (China) 99, 311–323.

Shi, Y.Q., Xi, Z.Y., Simayi, M., Li, J., Xie, S.D., 2020. Scattered coal is the largest source of ambient volatile organic compounds during the heating season in Beijing. Atmos. Chem. Phys. 20, 9351–9369.

Shrivastava, M., Cappa, C.D., Fan, J.W., Goldstein, A.H., Guenther, A.B., Jimenez, J.L., Kuang, C., Laskin, A., Martin, S.T., Ng, N.L., Petaja, T., Pierce, J.R., Rasch, P.J., Roldin, P., Seinfeld, J.H., Shilling, J., Smith, J.N., Thornton, J.A., Volkamer, R., Wang, J., Worsnop, D.R., Zaveri, R.A., Zelenyuk, A., Zhang, Q., 2017. Recent advances in understanding secondary organic aerosol: implications for global climate forcing. Rev. Geophys. 55, 509–559.

Song, Y.S., Lin, C.Q., Li, Y., Lau, A.K.H., Fung, J.C.H., Lu, X.C., Guo, C., Ma, J., Lao, X.Q., 2021. An improved decomposition method to differentiate meteorological and anthropogenic effects on air pollution: a national study in China during the COVID-19 lockdown period. Atmos. Environ. 250.

Sun, W., Shao, M., Granier, C., Liu, Y., Ye, C.S., Zheng, J.Y., 2018. Long-term trends of anthropogenic SO_2, NO_x, CO, and NMVOCs emissions in China. Earth Future 6, 1112–1133.

Sun, Y.L., He, Y., Kuang, Y., Xu, W.Y., Song, S.J., Ma, N., Tao, J.C., Cheng, P., Wu, C., Su, H., Cheng, Y.F., Xie, C.H., Chen, C., Lei, L., Qiu, Y.M., Fu, P.Q., Croteau, P., Worsnop, D.R., 2020. Chemical differences between PM_1 and $PM_{2.5}$ in highly polluted environment and implications in air pollution studies. Geophys. Res. Lett. 47, 10.

Wang, S., Su, H., Chen, C., Tao, W., Streets, D.G., Lu, Z., Zheng, B., Carmichael, G.R., Lelieveld, J., Poschl, U., Cheng, Y., 2020. Natural gas shortages during the "coal-to-gas" transition in China have caused a large redistribution of air pollution in winter 2017. Proc. Natl. Acad. Sci. U. S. A. 117, 31018–31025.

Wu, R., Xie, S., 2017. Spatial distribution of ozone formation in China derived from emissions of speciated volatile organic compounds. Environ. Sci. Technol. 51, 2574–2583.

Wu, W., Zhao, B., Wang, S., Hao, J., 2017. Ozone and secondary organic aerosol formation potential from anthropogenic volatile organic compounds emissions in China. J. Environ. Sci. (China) 53, 224–237.

Xu, W., Han, T., Du, W., Wang, Q., Chen, C., Zhao, J., Zhang, Y., Li, J., Fu, P., Wang, Z., Worsnop, D.R., Sun, Y., 2017. Effects of aqueous-phase and photochemical processing on secondary organic aerosol formation and evolution in Beijing,China. Environ. Sci. Technol. 51, 762–770.

Xu, W.Q., Sun, Y.L., Wang, Q.Q., Zhao, J., Wang, J.F., Ge, X.L., Xie, C.H., Zhou, W., Du, W., Li, J., Fu, P.Q., Wang, Z.F., Worsnop, D.R., Coe, H., 2019. Changes in aerosol chemistry from 2014 to 2016 in winter in Beijing: insights from high-resolution aerosol mass spectrometry. J. Geophys. Res.-Atmos. 124, 1132–1147.

Xu, L., Tsona, N.T., You, B., Zhang, Y., Wang, S., Yang, Z., Xue, L., Du, L., 2020. NO_x enhances secondary organic aerosol formation from nighttime γ-terpinene ozonolysis. Atmos. Environ. 225.

Zhai, S.X., Jacob, D.J., Wang, X., Shen, L., Li, K., Zhang, Y.Z., Gui, K., Zhao, T.L., Liao, H., 2019. Fine particulate matter ($PM_{2.5}$) trends in China, 2013-2018: separating contributions from anthropogenic emissions and meteorology. Atmos. Chem. Phys. 19, 11031–11041.

Zhang, Q., He, K., Huo, H., 2012. Policy: cleaning China's air. Nature 484, 161–162.

Zhang, J.K., Cheng, M.T., Ji, D.S., Liu, Z.R., Hu, B., Sun, Y., Wang, Y.S., 2016. Characterization of submicron particles during biomass burning and coal combustion periods in Beijing, China. Sci. Total Environ. 562, 812–821.

Zhang, Y.J., Tang, L.L., Croteau, P.L., Favez, O., Sun, Y.L., Canagaratna, M.R., Wang, Z., Couvidat, F., Albinet, A., Zhang, H.L., Sciare, J., Prevot, A.S.H., Jayne, J.T., Worsnop, D.R., 2017. Field characterization of the $PM_{2.5}$ aerosol chemical speciation monitor: insights into the composition, sources, and processes of fine particles in eastern China. Atmos. Chem. Phys. 17, 14501–14517.

Zhang, P., Chen, T., Liu, J., Liu, C., Ma, J., Ma, Q., Chu, B., He, H., 2019a. Impacts of SO_2, relative humidity, and seed acidity on secondary organic aerosol formation in the ozonolysis of butyl vinyl ether. Environ. Sci. Technol. 53, 8845–8853.

Zhang, Q., Zheng, Y., Tong, D., Shao, M., Wang, S., Zhang, Y., Xu, X., Wang, J., He, H., Liu, W., Ding, Y., Lei, Y., Li, J., Wang, Z., Zhang, X., Wang, Y., Cheng, J., Liu, Y., Shi, Q., Yan, L., Geng, G., Hong, C., Li, M., Liu, F., Zheng, B., Cao, J., Ding, A., Gao, J., Fu, Q., Huo, J., Liu, B., Liu, Z., Yang, F., He, K., Hao, J., 2019b. Drivers of improved $PM_{2.5}$ air quality in China from 2013 to 2017. Proc. Natl. Acad. Sci. U. S. A. 116, 24463–24469.

Zhang, X.Y., Xu, X.D., Ding, Y.H., Liu, Y.J., Zhang, H.D., Wang, Y.Q., Zhong, J.T., 2019c. The impact of meteorological changes from 2013 to 2017 on $PM_{2.5}$ mass reduction in key regions in China. Sci. China-Earth Sci. 62, 1885–1902.

Zhang, C., Liu, X.G., Zhang, Y.Y., Tan, Q.W., Feng, M., Qu, Y., An, J.L., Deng, Y.J., Zhai, R.X., Wang, Z., Cheng, N.L., Zha, S.P., 2021. Characteristics, source apportionment and chemical conversions of VOCs based on a comprehensive summer observation experiment in Beijing. Atmos. Pollut. Res. 12, 183–194.

Zhao, J., Du, W., Zhang, Y.J., Wang, Q.Q., Chen, C., Xu, W.Q., Han, T.T., Wang, Y.Y., Fu, P.Q., Wang, Z.F., Li, Z.Q., Sun, Y.L., 2017. Insights into aerosol chemistry during the 2015 China Victory Day parade: results from simultaneous measurements at ground level and 260 m in Beijing. Atmos. Chem. Phys. 17, 3215–3232.

Zhao, J., Qiu, Y.M., Zhou, W., Xu, W.Q., Wang, J.F., Zhang, Y.J., Li, L.J., Xie, C.H., Wang, Q.Q., Du, W., Worsnop, D.R., Canagaratna, M.R., Zhou, L.B., Ge, X.L., Fu, P.Q., Li, J., Wang, Z.F., Donahue, N.M., Sun, Y.L., 2019. Organic aerosol processing during winter severe haze episodes in Beijing. J. Geophys. Res.-Atmos. 124, 10248–10263.

Zhou, W., Gao, M., He, Y., Wang, Q., Xie, C., Xu, W., Zhao, J., Du, W., Qiu, Y., Lei, L., Fu, P., Wang, Z., Worsnop, D.R., Zhang, Q., Sun, Y., 2019. Response of aerosol chemistry to clean air action in Beijing, China: insights from two-year ACSM measurements and model simulations. Environ. Pollut. 255, 113345.